JOURNAL OF GUIDANCE, CONTROL, AND DYNAMICS
Vol. 19, No. 4, July–August 1996

Optimally Scaled $\mathcal{H}_\infty$ Full Information Control Synthesis with Real Uncertainty

Gary J. Balas* and Rick Lind†
University of Minnesota, Minneapolis, Minnesota 55455
and
Andy Packard‡
University of California, Berkeley, Berkeley, California 94720

An algorithm to synthesize optimal controllers for the scaled $\mathcal{H}_\infty$ full information problem with real and complex uncertainty is presented. The control problem is reduced to a linear matrix inequality, which can be solved via a finite dimensional convex optimization. This technique is compared with the optimal scaled $\mathcal{H}_\infty$ full information with only complex uncertainty and $D-K$ iteration control design to synthesize controllers for a missile autopilot. Directly including real parametric uncertainty into the control design results in improved robust performance of the missile autopilot. The controller synthesized via $D-K$ iteration achieves results similar to the optimal designs.

I. Introduction

MODERN control theory based on $\mathcal{H}_\infty$ optimal control has focused on the issue of robustness in control synthesis and analysis.' Unfortunately, the $\mathcal{H}_\infty$ norm alone often leads to a conservative estimate of robustness for structured uncertainty. The structured singular value μ was introduced as a measure of robustness in the presence of modeling uncertainty with performance specifications'; μ reduces the conservativeness of the $\mathcal{H}_\infty$ norm by accounting for the uncertainty structure in the analysis.

Consider two types of uncertainty: complex and real. Complex uncertainty is often used to represent unmodeled dynamics. Real uncertainty corresponds to errors in system parameters or coefficients of a plant model. The synthesis of output feedback controllers, robust to real parameter uncertainty, has been the focus of many researchers. Haddad and Bernstein[3] presented a maximum entropy approach using parameter-dependent Lyapunov functions and Popov's criterion to include real parameter uncertainty into the problem formulation. An alternative method using the Popov criterion is proposed by How and Hall.[4] They design controllers using a nonlinear search algorithm to optimize robustness and performance simultaneously.

$D-K$ iteration for μ synthesis, which is based on $\mathcal{H}_\infty$ control methods and μ analysis, was extended to directly include real parameter uncertainty by Young.[5] This requires the addition of a G scaling associated with the real uncertainty. The G scaling reduces the conservativeness of the resulting controllers to real perturbations. Safanov and Chiang[6] present a method for control design based on optimization techniques, which is similar to $D-K$ iteration. Their problem formulation incorporates parameter uncertainty into the optimization problem governing the control design process. All of these output feedback methods that account for real parametric uncertainty are not guaranteed to converge to a global optimum.

To find a globally optimal, robust controller for a plant with structured uncertainty, we consider a special case of the general output feedback problem, the full information problem. The full information problem provides the controller with direct measurement of the plant states and disturbances. Packard et al.[7,8] have shown for the $\mathcal{H}_\infty$ full information problem with linear, time-varying structured complex uncertainty that the optimal scalings and controller require solution of a single, convex optimization problem. Since the problem is convex, the global optimum of the scaled $\mathcal{H}_\infty$ norm is achieved, and the optimum controller is constant gain.

This paper extends the optimally scaled, $\mathcal{H}_\infty$ full information design method to account for real, time-varying parametric uncertainty.[7] These results build on the work presented in Ref. 8. The new results in this paper include the following.

1) The $\mathcal{H}_\infty$ full information, controller synthesis with real parametric uncertainty as a single linear matrix inequality is formulated. Convex optimization methods are used to solve the problem, resulting in a globally optimal controller.

2) The optimal controller is a constant, complex gain compensator, which can be realized as a dynamic system.

3) These results are applied to the design of a missile autopilot, and comparison with other control design methods is made.

In addition to its theoretical interest, the scaled $\mathcal{H}_\infty$ norm achieved provides a lower bound for an output feedback controller of the same order. This can be useful as a lower bound for μ synthesis with constant scalings.

Both scaled $\mathcal{H}_\infty$ full information control design techniques are applied to the synthesis of an autopilot for a nonlinear, pitch-axis model of a missile. These controllers are compared to an output feedback controller designed using $D-K$ iteration. The closed-loop systems are analyzed with respect to linear, time-invariant and time-varying parametric uncertainty, and nonlinear simulations are performed. Directly accounting for real parametric uncertainty in the design process leads to increased robustness of the closed-loop system to changes in angle of attack and Mach number. Note that the output feedback controller synthesized via $D-K$ iteration achieves robust performance levels similar to the optimally scaled $\mathcal{H}_\infty$ designs.

The following section provides a brief synopsis of results in the area of $\mathcal{H}_\infty$ control design and μ analysis and synthesis. The optimally scaled $\mathcal{H}_\infty$ full information problem is presented in Sec. III. Section IV integrates real parameter uncertainty into the optimally scaled, full information $\mathcal{H}_\infty$ problem and formulates the solution as a single linear matrix inequality. Two different formulations of the resulting controllers are presented in Sec. V.

A missile autopilot is used as an example to apply the optimally scaled full information $\mathcal{H}_\infty$ techniques and $D-K$ iteration for complex uncertainty. The nonlinear equations of motion for the pitch axis of a missile are given along with the control design objectives in Sec. VI. The three controllers are analyzed using the structured singular value (μ) with linear time-invariant and time-varying uncertainty and nonlinear simulations. Controllers optimized with respect

Received Nov. 28, 1994; revision received Oct. 15, 1995; accepted for publication Feb. 10, 1996.

*Assistant Professor, Department of Aerospace Engineering. Member AIAA.

†Graduate Student, Department of Aerospace Engineering; currently National Research Council Postdoctoral Research Fellow, NASA Ames—Dryden Flight Research Facility, MS 4840D/RC, Edwards Air Force Base, CA 93523-0273.

‡Associate Professor, Department of Mechanical Engineering.

to real parametric uncertainty show significant improvement in robustness when compared with the other designs.

II. Robust Control with Real/Complex Uncertainty

Define $x \in R^n$ as the vector of states, $z \in R^{n_e}$ as the vector of errors, $y \in R^{n_y}$ as the vector of measurements, $d \in R^{n_d}$ as the vector of disturbances, and $u \in R^{n_u}$ as the vector of control inputs. The state-space description of a linear time-invariant (LTI) plant can be represented as

$$\begin{bmatrix} \dot{x} \\ z \\ y \end{bmatrix} = \begin{bmatrix} A & B_1 & B_2 \\ C_1 & E_{11} & E_{12} \\ C_2 & E_{21} & E_{22} \end{bmatrix} \begin{bmatrix} x \\ d \\ u \end{bmatrix}$$

where $A \in R^{n \times n}$, $B_1 \in R^{n \times n_d}$, $B_2 \in R^{n \times n_u}$, $C_1 \in R^{n_e \times n}$, $C_2 \in R^{n_y \times n}$, and the E matrices are of appropriate dimensions. Define P as the Laplace transform of this system,

$$P(s) = \begin{bmatrix} P_{11}(s) & P_{12}(s) \\ P_{21}(s) & P_{22}(s) \end{bmatrix} = \begin{bmatrix} E_{11} & E_{12} \\ E_{21} & E_{22} \end{bmatrix} + \begin{bmatrix} C_1 \\ C_2 \end{bmatrix} (sI - A)^{-1} [B_1 \quad B_2]$$

and $S(P)$ as the set of all real, rational, proper controllers $K(s)$, which stabilize the closed-loop system. The incorporation of a controller into the system leads to the following linear fractional transformation (LFT)[9]:

$$F_l(P, K) = P_{11} + P_{12} K (I - P_{22} K)^{-1} P_{12}$$

This LFT represents the closed-loop transfer function with the lower loop of P closed with the controller K. To determine whether a closed-loop system can achieve a desired infinity norm performance, the following minimization problem can be posed as

$$\inf_{K \in S(P)} \| F_l(P, K) \|_\infty$$

This is an $\mathcal{H}_\infty$ optimal controller synthesis problem, which can be solved using well-known state–space methods.[1]

The structured singular value μ can be used to determine robustness of the closed-loop system to structured modeling uncertainty and the achievable performance level in the presence of real and complex uncertainty.[2,5,10] Uncertainty is defined using two types of blocks in the μ framework: repeated scalar and full block matrices. Let integers m, n, and p define the number of real scalar, complex scalar, and complex full blocks. Define integers $R_1, \ldots, R_m$ such that the ith repeated scalar block of real parametric uncertainty is of dimension $R_i \times R_i$. Define similar integers $C_1, \ldots, C_n$ to denote the dimension of the complex repeated scalar blocks. The structured uncertainty description **A** is assumed to be norm bounded and belonging to the following set:

$$\mathbf{A} = \{ A = \operatorname{diag}\left(\delta_1^R I_{R_1}, \ldots, \delta_m^R I_{R_m}, \delta_1^C I_{C_1}, \ldots, \delta_n^C I_{C_n}, \Delta_1, \ldots, \Delta_p\right) : \delta_i^R \in R, \delta_i^C \in C, \Delta_i \in C^{c_i \times c_i} \}$$

Real parametric uncertainty is allowed to enter the problem as a scalar or repeated scalar block. Complex uncertainty enters the problem as a scalar, repeated scalar, or full block. The structured singular value μ is defined as

$$\mu_{\mathbf{\Delta}}(M) = \frac{1}{\min_{\mathbf{\Delta}} \{ \bar{\sigma}(\Delta) : \det(I - M\Delta) = 0 \}}$$

with $\mu_{\mathbf{\Delta}}(M) = 0$ if no **A** exists such that $\det(I - MA) = 0$. Note that the value of μ depends on the block structure of **A**. Upper and lower bounds for μ have been derived that utilize two sets of structured scaling matrices, D and G. These scaling matrices are similar in structure to the uncertainty blocks. Define the scaling set D as

$$\mathcal{D} = \left\{ D = \operatorname{diag}\left(D_1^R, \ldots, D_m^R, D_1^C, \ldots, D_n^C d_1^c I_{c_1}, \ldots, d_p^c I_{c_p}\right) : D_i^R \in C^{R_i \times R_i}, D_i^C \in C^{C_i \times C_i}, d_i \in C \right\}$$

The set of scalings $\mathcal{G}$ affect only the real parametric uncertainty blocks,

$$\mathcal{G} = \left\{ G = \operatorname{diag}(G_1, \ldots, G_m, 0, \ldots, 0) : G_i \in C^{R_i \times R_i} \right\}$$

An upper bound for μ with real and complex uncertainty[11,12] is defined as

$$\mu(M) \le \inf_{\substack{D \in \mathcal{D} \\ G \in \mathcal{G}}} \bar{\sigma}\left[(DMD^{-1} + jG)(I + G^2)^{\frac{1}{2}} \right] \le \inf_{D \in \mathcal{D}} \bar{\sigma}(DMD^{-1})$$

Similarly, a lower bound for mixed μ can be defined.[1] The mixed μ upper and lower bounds reduce to the well-known complex μ bounds when there are no real uncertainty blocks.

The structured singular value provides a measure of robustness in the presence of the defined structured uncertainty. The D and G matrices are allowed to vary with frequency for LTI uncertainty. These scalings are restricted to be constant when computing robustness in the presence of linear time-varying (LTV) uncertainty.[13] Rate bounds on the time rate of change of the uncertainty can be incorporated into the analysis but are not addressed in this paper.[14]

The objective of control design is to maximize robust performance, which corresponds to minimizing μ in this framework. An approach to output feedback control design, which minimizes complex μ, is called D–K iteration. This technique is used to synthesize output feedback controllers for the missile autopilot example. D–K iteration tries to achieve the desired robust performance objectives by integrating $\mathcal{H}_\infty$ control design with complex μ analysis.[1,11,15] D–K iteration alternately minimizes the complex μ upper bound with respect to K or D holding the other variable constant. This technique has been applied with great success to a variety of aerospace applications despite a lack of guarantee to reach the global optimum.[15–17] A more detailed discussion of D–K iteration can be found in Refs. 9 and 15. An approach to minimizing the μ upper bound for the full information case is presented in the following section.

III. Optimal, Full Information Controllers

An algorithm to compute the optimally scaled, $\mathcal{H}_\infty$ full information (FI) controller for a system with LTV uncertainty was presented by Packard et al.[7,8] This algorithm considers the synthesis problem with constant D scalings included to allow infinitely fast time variation in the complex uncertainty. This section outlines this synthesis procedure and presents the main theorem given in Ref. 7.

The open-loop system considered is a continuous-time plant. The controller is provided with direct measurement of the states and disturbances and is called the FI plant. The closed-loop $\mathcal{H}_\infty$ norm condition is shown to be equivalent to a maximum singular value condition involving the constant matrix form of the discretized FI plant. The following theorem demonstrates this equivalency.[7]

Theorem 1. Given the full information plant $P_{fi}(s)$ and the constant matrix discrete-time plant $\hat{P}_{fi}$ along with the set $\mathbf{D}$ of scaling matrices, then the following are equivalent.

1) There exists $D \in \mathbf{D}$ and stabilizing $K \in S(P_{fi})$ such that

$$\left\| D^{\frac{1}{2}} F_l[P_{fi}(s), K] D^{-\frac{1}{2}} \right\|_\infty < 1$$

2) There exists $D \in \mathcal{D}$ and stabilizing $K \in S(P_{fi})$ along with real $X = X^T > 0$ such that with $Z = \operatorname{diag}(X, D)$

$$\bar{\sigma}\left(Z^{\frac{1}{2}} F_l(\hat{P}_{fi}, K) Z^{-\frac{1}{2}} \right) < 1$$

The proof, given in Ref. 7, is based on standard linear algebra arguments and properties of LFT to equate these conditions.

The resulting constant matrix problem has two scaling matrices, D and X. D is the original constant matrix that scales the plant inputs and outputs. X is the symmetric positive definite solution matrix in the Riccati formulation of the $\mathcal{H}_\infty$ problem. It scales the inputs and outputs of the discrete-time state equation. The X matrix is included in the singular value test to restrict the eigenvalues of the discrete-time state matrix to be less than one to guarantee stability.

Now perform a change of variables. Denote the entries of the discrete-time plant as (R, U, V, T), and introduce Q to replace $K(I + TK)^{-1}$ in the closed-loop LFT for notational convenience,

$$F_l(\hat{P}_{fi}, K) = R + UK(I + TK)^{-1}V = R + UQV$$

A variant of Parrott's theorem is used to formulate two maximum eigenvalue conditions equivalent to the constant matrix singular value condition introduced in Theorem 1. The resulting eigenvalue condition is presented in Lemma 2.

Lemma 2. Given the discrete-time plant $\hat{P}_{fi}$, formulate the closed-loop LFT as $F_l(\hat{P}_{fi}, K) = R + UQV$ and define $U_\perp$ such that $[U \;\; U_\perp]$ is invertible and $U^T U_\perp = 0$. Then

$$\inf_{\substack{Q \in S(P) \\ Z \in \mathcal{Z}}} \bar{\sigma}\left[Z^{\frac{1}{2}}(R + UQV)Z^{-\frac{1}{2}} \right] < 1$$

if and only if there exists $Z \in \mathcal{Z}$ such that

$$\bar{\lambda}\left[U_\perp^T (RZ^{-1}R^T - Z^{-1})U_\perp\right] < 0$$

The proof follows directly from Parrott's theorem.[7,18] There is an additional eigenvalue condition involving the matrix V and a perpendicular component $V_\perp$ defined similar to $U_\perp$. The V matrix in the LFT of the closed-loop system with the FI plant is square and invertible and so $V_\perp$ is null. The maximum eigenvalue condition utilizing this variable is automatically satisfied. The remaining maximum eigenvalue condition is a linear matrix inequality (LMI) with the scaling matrix as the free parameter.

The $\mathcal{H}_\infty$ synthesis problem for the continuous-time FI system is thus reduced to a single constant matrix maximum eigenvalue problem using elements of the discrete-time FI system. The following theorem summarizes the synthesis procedure for systems with infinitely fast varying LTV structured, complex uncertainty.[7,8]

Theorem 3. Given the n-state full information plant P_{fi} and the set $\mathcal{D}$,

$$P_{fi} = \begin{bmatrix} E_{11} & E_{12} \\ 0 & 0 \\ I_h & 0 \end{bmatrix} + \begin{bmatrix} C_1 \\ I_n \\ 0 \end{bmatrix} (sI - A)^{-1} [B_1 \quad B_2]$$

Define the following.

1) The augmented scaling matrices $\mathcal{Z}$

$$\mathcal{Z} = \left\{ \begin{bmatrix} X & 0 \\ 0 & D \end{bmatrix} : X \in \mathbf{R}^{n \times n}, X = X^T > 0, D \in \mathcal{D} \right\}$$

2) Also, $a > 0$, so that $(I - \alpha A)$ is invertible.

3) Matrices R, U

$$R = \begin{bmatrix} (I + \alpha A)(I - \alpha A)^{-1} & \&(I \quad -\alpha A)^{-1} B_1 \\ \sqrt{2\alpha} C_1 (I - \alpha A)^{-1} & E_{11} + C_1 (I - \alpha A)^{-1} B_1 \end{bmatrix}$$

$$U = \begin{bmatrix} \sqrt{2\alpha}(I - \alpha A)^{-1} B_2 \\ D_{12} + C_1 (I - \alpha A)^{-1} B_2 \end{bmatrix}$$

4) Matrix $U_\perp$ such that $[U \;\; U_\perp]$ is orthogonal.

Then, there exists a matrix $K \in S(P)$ and a constant $D \in \mathcal{D}$ such that

$$\left\| D^{\frac{1}{2}} F_l(P_{fi}, K) D^{-\frac{1}{2}} \right\|_\infty < 1$$

if and only if the following convex set is nonempty:

$$\left\{ Z \in \mathcal{Z} : \lambda_{\max}\left[U_\perp^T (RZR^* - \alpha^2 Z) U_\perp \right] < 0 \right\} \neq \{\emptyset\}$$

The optimal controller gains may be computed by scaling the continuous-time plant with the constant $\mathcal{D}$ matrices and utilizing standard $\mathcal{H}_\infty$ state–space algorithms given in Ref. 1 or the controller formulation algorithms given in Sec. V.

IV. Optimal FI Synthesis for Real/Complex Uncertainty

The synthesis algorithm for systems with complex uncertainty can be extended to include systems with real parametric uncertainty using the real/complex μ upper bound. The procedure is similar to the FI synthesis for complex uncertainty. The algebraic Riccati equation associated with the $\mathcal{H}_\infty$ norm condition for the continuous-time plant is again shown to be equivalent to a constant matrix singular value condition involving the discrete-time plant. The constant scaling matrices X and D are included in the problem to ensure stability and reduce conservativeness. An additional set of constant scalings $\mathcal{G}$ are included in the formulation to reduce conservativeness of the μ upper bound for real uncertainty.

A variant of Parrott's theorem is again used to equate the constant matrix maximum singular condition to a pair of maximum eigenvalue conditions. One of these conditions is automatically satisfied for the FI plant. Consider the upper bound for mixed μ for a constant matrix[8,11]:

$$\mu(R + UQV) \leq \bar{\sigma}\left\{ [D(R + UQV)D^{-1} + jG](I + G^2)^{-\frac{1}{2}} \right\}$$

$$\leq \bar{\sigma}(\bar{R} + \bar{U}Q\bar{V})$$

where

$$\bar{R} = (DRD^{-1} + jG)(I + G^2)^{-\frac{1}{2}}, \qquad \bar{U} = DU$$

$$\bar{V} = VD^{-1}(I + G^2)^{-\frac{1}{2}}$$

The upper bound in the variables $\mathbf{R}, \bar{U}$, and $\bar{V}$ can be shown to be equivalent to a single maximum eigenvalue function using the same procedure outlined in Ref. 7:

$$\bar{\lambda}\left[\bar{U}_\perp^* (\bar{R}\bar{R}^* - I)\bar{U}_\perp\right]$$

$$= \bar{\lambda}\left\{ U_\perp^* D^{-1} [(DRD^{-1} + jG)(I + G^2)^{-1} \right.$$

$$\left. x\,(D^{-1}R^*D - jG) - I] D^{-1} U_\perp \right\}$$

$$= \bar{\lambda}\left\{ U_\perp^* [R\bar{D}^{-2}R^* + j(\bar{G}R^* - R\bar{G}) - \bar{D}^{-2}] U_\perp \right\}$$

where

$$D = D^{-1}(I + G^2)^{-1} D^{-1} \in \mathcal{D}$$

$$G = D^{-1} G (I + G^2)^{-1} D^{-1} \in \mathcal{G}$$

These equations lead to the following lemma, which parallels Theorem 3 for systems with complex and real uncertainty.

Lemma 4. Given the continuous-time, full information plant $P_{fi}(s)$ with some uncertainty description $\mathbf{A}$, define the discrete-time plant $\hat{P}_{fi}$ such that for some stabilizing controller K, $F_l(\hat{P}_{fi}, K) = R + UQV$ where R and U are explicitly given in Theorem 3. There exists a stabilizing controller $K \in S(P_{fi})$ such that $\mu[F_l(P_{fi}(s), K)] < 1$ if there exists $\bar{D} \in \mathcal{D}$ and $\bar{G} \in \mathcal{G}$ such that

$$\bar{\lambda}\left\{ U_\perp^* [R\bar{D}^{-2}R^* + j(\bar{G}R^* - R\bar{G}) - \bar{D}^{-2}] U_\perp \right\} < 0$$

The maximum eigenvalue condition to be solved in Lemma 4 is a single convex LMI in the matrix variables D and G. The optimal scaling matrices are computed along with the achievable robustness in the presence of the uncertainty set. The following section will demonstrate how to compute the optimal controller given the robustness level and associated scaling matrices.

Lemma 4 along with Theorem 3 demonstrate how to synthesize optimal, FI controllers for plants with complex and real uncertainty. The elements of the continuous-time plant are used to formulate constant R and U matrices. An LMI is formulated involving these matrices to compute the optimal scaling matrices. The optimal controller is computed given these optimal scalings using the techniques presented in the next section.

The free parameters used in the optimization are the elements of the scaling matrices D and G. Symmetry of the scaling matrices

is used to reduce the number of elements for an $n \times n$ matrix to $\frac{1}{2}n(n+1)$ parameters. The missile autopilot control design with real and complex uncertainty presented in this paper formulates an LMI with 172 free parameters in the optimization. The resulting convex optimization is solved using the ellipsoid algorithm.[19,20]

V. Controller Formulation

Two ways are presented to compute the optimal scaled, real/complex FI controller directly from the scaling matrices produced by the convex optimization algorithm given in Lemma 4. The original upper bound scaling matrices D and G are computed from the modified scaling matrices $\bar{D}$ and $\bar{G}$ given in Lemma 4:

$$G = \bar{D}^{-\frac{1}{2}} G \bar{D}^{\frac{1}{2}} \qquad D = (I + G^2)^{-\frac{1}{2}} \bar{D}^{-\frac{1}{2}}$$

Therefore, the elements of the scaled closed-loop formulation $R + \bar{U} Q \bar{V}$ are known except for the unknown Q. Q is selected such that the maximum singular value of the closed-loop system is less than 1:

$$\bar{\sigma}(\bar{R} + \bar{U} Q \bar{V}) < 1$$

This proper Q used to parametrize the controller is computed using the Moore–Penrose pseudoinverse and the D and G scalings (a general parametrization of Q is given in Ref. 18):

$$Q = -[(\bar{U}^* \bar{U}) \backslash \bar{U}] \bar{R} (I + G^2)^{\frac{1}{2}} D V^{-1}$$

The controller K is computed with these elements based on the parameterization of the controller as an LFT, to form the system $R + UQV$:

$$K = (I + QT)^{-1} Q$$

The resulting controller is a stabilizing, constant gain controller guaranteed to achieve the optimal closed-loop norm for the FI system.

This optimal constant gain controller may have complex entries. The imaginary components arise because both sets of scaling matrices are allowed to be complex. A complex gain feedback is physically unrealizable since it leads to imaginary signals. A dynamic controller, having real entries, may be formulated from the entries of the complex gain controller that is guaranteed to achieve a norm at least as low as that of the complex gain controller.[21]

Consider the FI plant and the constant complex gain controller K_C derived previously. The complex gains result in complex states and errors in the closed-loop system. Separate the controller into real and complex entries for the state and disturbance feedback, where K_{R_x} and K_{R_d} correspond to the real gains and K_{I_x} and K_{I_d} correspond to the imaginary gains of the state and disturbance feedback, respectively; $K_C = [K_{R_x} \;\; K_{R_d}] + j[K_{I_x} \;\; K_{I_d}]$.

It is straightforward to calculate the closed-loop system from disturbances to the real and complex parts of the errors. The state–space description of this system will have complex entries, which is undesirable. Consider a state–space formulation of the closed-loop system that treats the real and complex parts of the states and errors as separate signals,

$$F_l(P_{fi}, K_C) = \left[\begin{array}{cc|c} A + B_2 K_{R_x} & -B_2 K_{I_x} & B_1 + B_2 K_{R_d} \\ B_2 K_{I_x} & A + B_2 K_{R_x} & B_2 K_{I_d} \\ \hline C_1 + D_{12} K_{R_x} & -D_{12} K_{I_x} & D_{11} + D_{12} K_{R_x} \\ D_{12} K_{I_x} & C_1 + D_{12} K_{R_x} & D_{12} K_{I_d} \end{array}\right]$$

The first set of states in this formulation are the real components of the actual states and the second set of states are the imaginary components. The real components of the errors are the first set of outputs, whereas the imaginary components of the errors are the second set of outputs. It is possible to formulate a real, dynamic controller that achieves a closed-loop norm at least as low as the closed-loop system formed with the preceding complex, constant gain controller. Consider the following dynamic, real compensator:

$$K_R(s) = \left[\begin{array}{c|cc} A + B_2 K_{R_x} & B_2 K_{I_x} & B_2 K_{I_d} \\ \hline -K_{I_x} & K_{R_x} & K_{R_d} \end{array}\right]$$

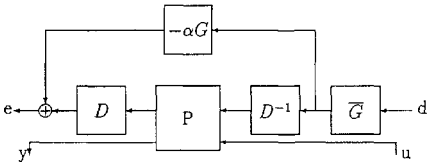

Fig. 1 Scaled open-loop system.

The dynamic controller is of the same order as the plant. This state–space controller presents a more attractive formulation in that it is physically realized. The closed-loop systems $F_l(P_{fi}, K_C)$ and $F_l[P_{fi}, K_R(s)]$ are equivalent except for the imaginary component of the error signals with the K_C controllers. The $\mathcal{H}_\infty$ norm achieved with $K_R(s)$ is guaranteed to be no greater than with K_C.

Lemma 5. Given the full information plant P_{fi} and stabilizing controllers K_C, $K_R(s)$ defined earlier, then $\|F_l[P_{fi}, K_R(s)]\|_\infty \leq \|F_l(P_{fi}, K_C)\|_\infty$.

Proof. The two closed-loop systems are identical excepting errors of the system with K_C contains an imaginary part. The two-norm of the complex error is less than the two-norm of the purely real error,

$$\|e_R + j e_I\|_2 = \sqrt{\int_0^\infty \left[e_R^2(t) + e_I^2(t)\right] \mathrm{d}t}$$

$$\geq \sqrt{\int_0^\infty e_R^2(t)\, \mathrm{d}t}$$

$$\geq \|e_R\|_2$$

$$\|F_l[P_{fi}, K_R(s)]\|_\infty = \frac{\|e_R\|_2}{\|d\|_2} \leq \frac{\|e_R + j e_I\|_2}{\|d\|_2} \leq \|F_l(P_{fi}, K_C)\|_\infty$$

It was shown by Rotea and Khargonekar that including dynamics in the state-feedback law does not lead to a lower norm value.[22,23] Therefore, an alternative formulation,[5] allows an indirect calculation of an optimal, constant gain controller. The controller is synthesized using a single D, G–K iteration. This method involves computing the optimal D and G matrices and appending D with the identity matrix and G with zeros. The open-loop plant is scaled with these matrices with the appended identity and zeros scaling the controller feedback measurements to form the optimally scaled open-loopplant $\tilde{P} = (D P_{fi} D^{-1} + G)(I + G^2)^{1/2}$. The optimal, constant gain FI $\mathcal{H}_\infty$ controller is synthesized for the optimally scaled open-loop plant using the techniques in Refs. 1 and 15. Given the scalings D and G, define $G = (I + G^2)^{-1/2}$. The open-loop plant is scaled as shown in Fig. 1.

VI. Missile Example

A. Missile Model

We will apply these optimally scaled $\mathcal{H}_\infty$ techniques to the design of a longitudinal autopilot for a missile flying between Mach 2 ard 3 at 20,000 ft. For comparison, an output feedback controller is synthesized using D–K iteration for the same system. The missile equations of motion and performance objectives are taken from Refs. 17, 24, and 25. The nonlinear state equations for the missile are

$$\dot{\alpha} = f_1(\alpha, q, M) = \frac{\cos^2(\alpha)}{\text{mass} \times U} F_z + q$$

$$\dot{q} = f_2(\alpha, q, M) = M_y / I_y$$

where

d	= diameter, 0.75 ft
F_z	$= \mathrm{sgn}(\alpha) C_n(\lvert\alpha\rvert, \delta) QS$, lb
g	= acceleration because of gravity, 32.2 ft/s^2
I_y	= pitch moment of inertia, 182.5 slug-ft^2
M	= Mach number of the missile, 2–3
M_y	$= \mathrm{sgn}(\alpha) C_m(\lvert\alpha\rvert, \delta) QSd$, ft-lb
mass	= mass of missile, 13.98 slug

Q = dynamic pressure, $0.7 \times \rho \times M^2$ lb/ft^2
q = pitch rate, radls
S = reference area, 0.44 ft^2
ss = speed of sound at 20,000 ft, 1036.4 ft/s
u = along missile centerline, $V \times \cos(\alpha)$, ft/s
V = velocity of missile, $M \times ss$, ft/s
α = angle-of-attack, rad
δ = tail fin deflection, rad
ρ = static pressure at 20,000 ft, 973.3 lb/ft^2

The aerodynamic coefficients C_n and C_m are given by the following polynomial expressions:

$$\begin{bmatrix} C_n \\ C_m \end{bmatrix} = \begin{bmatrix} 1.03 \times 10^{-4} & -9.45 \times 10^{-3} & -0.17 * \left[1 + \frac{1}{3}(3 - M)\right] & -0.34 \\ 2.15 \times 10^{-4} & 1.95 \times 10^{-2} & 0.051 * \left[1 + \frac{8}{3}(M - 3)\right] & -0.206 \end{bmatrix} \begin{bmatrix} |\alpha|^3 \\ \alpha^2 \\ |\alpha| \\ \delta \end{bmatrix}$$

These values are representative of the missile traveling between Mach 2 and 3 at an altitude of 20,000 ft. Typical maneuvers for this missile result in angle-of-attack values that range between -10 and 10 deg. These nonlinear equations are linearized about trim operating points and a state–space model of the missile, which is a function of angle of attack a, and Mach number M is derived. A linear fractional description of this dependence is used to define the control design model. There are two uncertainty parameters to account for the changes in angle-of-attack and six uncertainty parameters to account for Mach. The LFT missile model is included in the Appendix.

The poles of the pitch axis missile range from two stable, lightly damped roots at $-1.32 \pm j7.73$ rad/s at $a = 10$ deg to a stable and unstable root at $+15.13$ and -12.6 rad/s with the missile at $\alpha = 0$ deg. Therefore, to stabilize the airframe, the closed-loop bandwidth must be greater than 15.13 rad/s. A more detailed description of the missile model is presented in Refs. 24 and 25.

B. Control Objectives

It is desired to synthesize a single controller to track commanded acceleration maneuvers with a steady-state error of less than 10%, a time constant of less than 0.4 s, and a step response overshoot of less than 20%. The tail fin deflection is limited to 25 deg and the tail-deflection rate to 40 deg/s/g given f20-g acceleration commands. The controller is to provide performance over a range of ± 10-deg angle of attack and missile velocities between Mach 2 and 3. The controller must avoid saturating the tail-deflection actuator rate capabilities and destabilizing unmodeled high-frequency flexible body modes of the missile.

Traditional autopilots are gain scheduled over the flight regime. The approach used here is to treat the plant variations resulting from changes in Mach number M and angle-of-attack α as uncertainty. The robust control design techniques presented are used to compute a single controller that achieves stability and performance over the range of variations. **A** block diagram of the control problem formulation is shown in Fig. 2.

The tracking objective corresponds to a weighted H_∞ norm on the acceleration tracking error. The performance weighting function

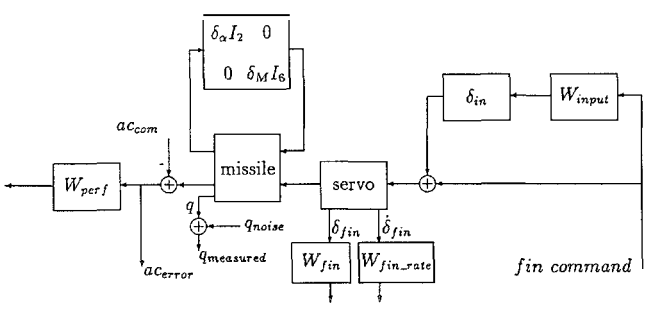

Fig. 2 Open-loop missile block diagram.

used in the designs is $W_{perf} = 0.15(s + 30)/(s + 0.3)$. Weightings are included on the actuator tail fin deflection angle $W_{fin} = 19$ and rate $W_{fin\_rate} = 1$. These weightings are used to limit the magnitudes of these signals to the desired performance goals. Noise on the pitch rate measurement, $q_{noise} = 10^{-3}$, is included in the design of the output feedback controller to satisfy rank conditions.

The actuator used in this missile is not of very high quality. This is reflected in the problem formulation with a multiplicative input uncertainty, denoted by $W_{input} = 1.5(s + 2)/(s + 80)$. The uncertainty weight indicates that the actuator model has approximately 25% error at 15 rad/s (the location of one of the unstable missile poles) and as much as 100% uncertainty at 71 rad/s. The missile and actuator models are given in the Appendix. Stabilization of the pitch-axis missile model is the driving constraint in this control problem.

C. Control Designs

There are three uncertainty blocks in the control problem, as seen in Fig. 2. The first is a repeated scalar uncertainty parameter δ_α. It accounts for variations in angle of attack of the vehicle and is repeated twice. The second uncertainty parameter δ_M is repeated six times and accounts for the range of Mach variation allowed in the system. Here δ_α and δ_M are variables associated with the physical system and, thus, are necessarily real quantities. A full, complex scalar uncertainty block Δ_{in} is included to model input uncertainty. The performance block has three inputs and one output. The uncertainty block structure is

$$\mathbf{\Delta} = \text{diag}\{\delta_\alpha I_{2\times 2}, \delta_M I_{6\times 6}, \Delta_{in}\}$$

The a and Mach variations δ_α and δ_M are LTV uncertainties. Here, δ_α and δ_M are defined such that 6, varying between ± 1 implies that the angle of attack a varies between ± 10 deg and δ_M varying between ± 1 implies the missile velocity M varies between Mach 2 and 3. Mach number and angle of attack are always real quantities, and so the associated uncertainty parameters are treated as real. The input uncertainty parameter contains magnitude and phase information and is treated as complex, time-invariant uncertainty.

Two full information missile autopilots are synthesized using the techniques described. The first controller treats all uncertainty in the synthesis process as complex. This controller, denoted K_{fic}, was used in Ref. 26 to compare various control design methods for systems with complex uncertainty. The second controller, denoted K_{fir}, is synthesized by directly accounting for real parametric a and Mach uncertainty and treating A, , as a complex uncertainty.

An output feedback controller is also designed using D–K iteration. The measurement signals feedback to the controller are the difference between the commanded and sensed acceleration and the pitch rate of the missile. The output feedback controller, denoted K_{of}, was of order 23 after three D–K iterations. Balanced realization model reduction techniques are used to reduce the controller order to 7. Controllers K_{fic} and K_{of} are synthesized treating the angle-of-attack variations δ_α and Mach number variation δ_M as complex perturbations. K_{fir} treats 6, and δ_M as real perturbations. The state–space descriptions of K_{fic}, K_{fir}, and K_{of} are presented in the Appendix.

D. Analysis/Simulations

Robust stability with time-invariant uncertainty may be analyzed for the linearized plant model for each controller using the μ-Analysis and Synthesis Toolbox." Calculating the upper and lower bound robust stability μ for the given time-invariant uncertainty structure leads to the results in Fig. 3. Treating δ_α, δ_M, and Ai, as complex perturbations leads to peak μ values greater than 1

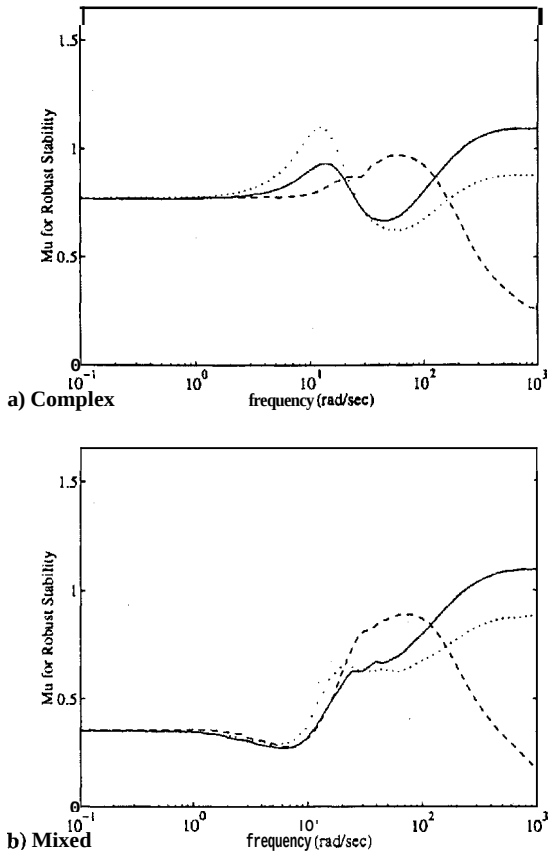

Fig. 3 Robust stability μ plots with linear, time-invariantuncertainty: ——, K_{fic}; . . ., K_{fir}; and – – –, K_{of}.

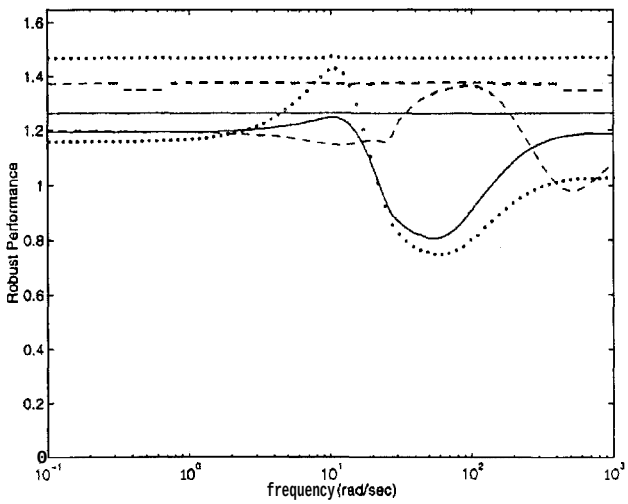

Fig. 4 Robust performance complex μ for LTI uncertainty (lower line) and LTV uncertainty (upper line): ——, K_{fic}; . . ., K_{fir}; and – – –, K_{of}.

for the FI controllers. The μ values achieved are 1.2 for K_{fic}, 1.09 for K_{fir}, and 0.97 for K_{of}. The peak μ values are reduced for each system by treating the Mach number and angle-of-attack variations as real quantities. Analyzing robust stability with δ_M and δ_α treated as LTI real uncertainties results in μ values of 1.08 for K_{fic}, 0.88 for K_{fir}, and 0.89 for K_{of}.

Robust stability for the optimal, FI controller for complex uncertainty, K_{fic} is driven by the input uncertainty weight. This is the dominate uncertainty above 100 radls where the robust stability μ value is the highest. Robust stability at high frequency was not achieved for this controller because of the optimization procedure focusing on the controller crossover region, *8–20* radls. Recall that the controller bandwidth must exceed 15 radls to stabilize the unstable pitch-axis mode. The robust performance objective could

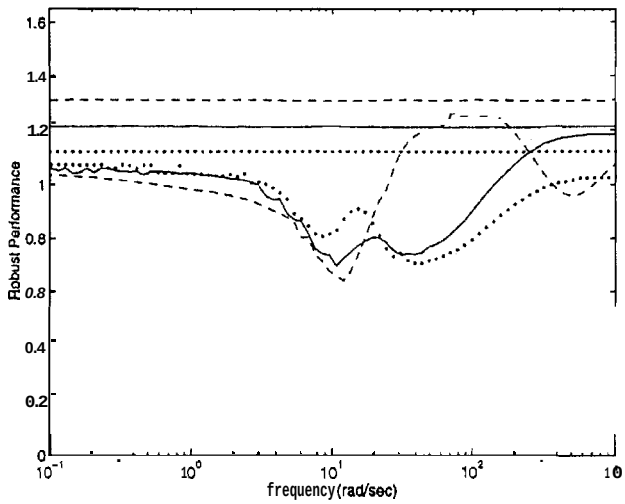

Fig. 5 Robust performance mixed μ for LTI uncertainty (lower line) and LTV uncertainty (upper line): ——, K_{fic}; . . ., K_{fir}; and – – –, K_{of}.

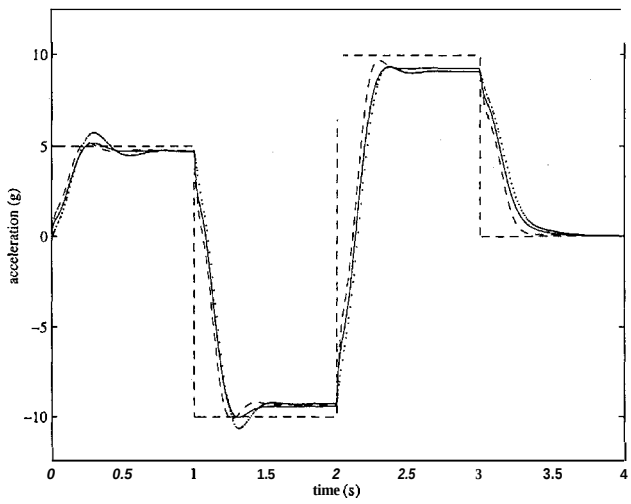

Fig. 6 Missile autopilot nonlinear simulation: ——, K_{fic}; . . ., K_{fir}; and – – –, K_{of}.

not be achieved in the 8–20-radls-frequency range; therefore, the optimization technique did not try to reduce the H_∞ norm in other frequency ranges. K_{fir} directly accounts for the real uncertainty in the system during the design process, which resulted in improved stability robustness of the closed-loop system.

The nominal performance is 0.61 for K_{fic}, 0.62 for K_{fir}, and 0.71 for the output feedback controller K_{of}. The weighted norm of the nominal performance less than 1 indicates that all the controllers achieve the desired performance objectives on the nominal system.

The robust performance μ for each controller with linear, time-invariant uncertainty is shown in Figs. 4 and 5. Treating S,, S,+,, and A;, as complex, time-invariant uncertainty leads to a peak μ value of 1.28 for K_{fic} 1.43 for K_{fir}, and 1.41 for K_{of}, respectively, as seen in Fig. 4. Computing μ with Mach number and angle-of-attack variations treated as real time-invariant quantities leads to a peak value of 1.16 for K_{fic}, 1.07 for K_{fir}, and 1.28 for K_{of}; see Fig. 5.

The robust performance μ plots for K_{fir} indicate there is an improvement in robustness by designing the controller to account for real uncertainties. The synthesis process for K_{fic} focused on the peak complex μ value around 15 radls and did not attempt to reduce the norm at other frequencies. The LTI, real/complex robust performance μ plot (Fig. *5)* shows that the peak value for K_{fic} occurs at frequencies above 100 radls where the input uncertainty dominates. Since the α and Mach variations no longer drive the controller synthesis problem when they are treated as real, the controller K_{fir} is able to concentrate on lowering the value of μ at high frequency.

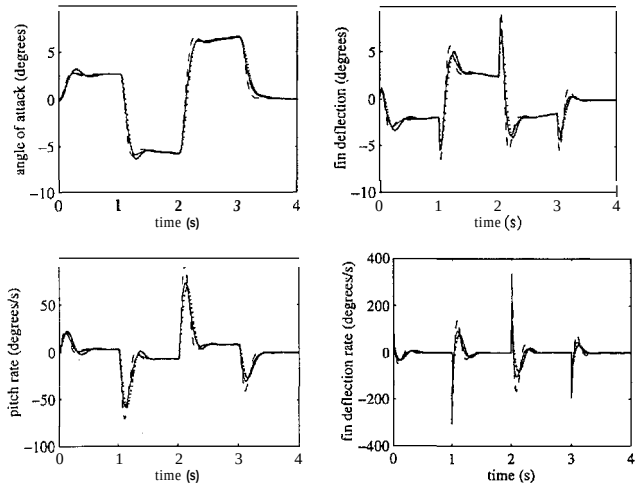

Fig. 7 Missile autopilot nonlinear simulation: ——, K_{fic}; ···, K_{fir}; and – – –, K_{of}.

The LTI, robust performance plots (Figs. 4 and 5), show that the optimal, FI controllers achieve a lower μ value than the controller designed using $D-K$ iteration. K_{fir} and K_{fic} achieve robust performance μ values 10–20% less than K_{of} for LTI uncertainty treated as either all complex or real and complex. The nominal performance results are similar. The complex robust stability plot, however, shows that the FI μ values are greater than for the output feedback system. This is not a contradiction, because the robust performance μ upper bound is being optimized rather than robust stability.

K_{fic} is unable to meet the desired robustness and performance objectives even for LTI uncertainty. Controller K_{fir} is close to meeting the desired robustness and performance objectives. The peak μ value is only 7% from the desired goal. We found that a reduction to 1/1.07 or 94% of the amount of input uncertainty results in this controller achieving the K_{fir} robust performance objective for the mixed LTI uncertainty.

The robust performance of the closed-loop systems can also be analyzed treating the angle-of-attack and Mach variations as time-varying uncertainties. This is important because a and M vary with time. They are accounted for in the optimal, scaled $\mathcal{H}_\infty$ FI control designs as infinitely fast, time-varying perturbations. Treating the angle-of-attack and Mach variations as complex, time-varying perturbations leads to robustness values of 1.26 for K_{fic}, 1.47 for K_{fir}, and 1.38 for K_{of}. Treating δ_α and δ_M as real, time-varying perturbations leads to robustness values of 1.21 for K_{fic}, 1.12 for K_{fir}, and 1.3 for K_{of}. These results correspond to the straight lines in Figs. 4 and 5.

Note that K_{fic} and K_{of} actually achieve better robustness than K_{fir} when all uncertainties are treated as complex. Again, this is not a contradiction, because K_{fir} is computed to lower the robustness measure when a and Mach uncertainties are treated as real, LTV perturbations. K_{fic} and K_{of} are optimized for complex uncertainties; hence, they are able to achieve a lower complex μ value. The robust performance μ value for K_{fir} is lower than K_{fic} and K_{of} when 6, and δ_M are treated as real LTV uncertain parameters. K_{fir} was synthesized to be the optimal, FI controller for LTV real parametric uncertainty for the given uncertainty structure. The robust performance values of K_{fic} and K_{of} are improved when these parameters are allowed to be real, but are at least 10% higher than K_{fir}.

Robust performance for the controllers is not greatly affected by the time-varying nature of the 6, and δ_M uncertainty parameters. The robustness for each controller is approximately 10% less for complex LTI uncertainty as compared to complex LTV uncertainty. The μ values show a similar relationship for real LTI and LTV uncertainty. The closeness of the LTI and LTV μ values indicate that allowing the a and M parameters to vary infinitely fast is not overly conservative. The LTV uncertainty increased μ slightly with robust stability still the driving constraint in the problem.

Time responses for a nonlinear simulation with the three controllers are presented in Figs. 6 and 7. A series of acceleration step commands of varying magnitudes are input to the missile. The time response plot of the vehicle's acceleration, commanded acceleration, tail fin deflection angle, and rate for all controllers are shown in Figs. 6 and 7. Mach number is a commanded variable in the nonlinear simulations. Mach is decreased linearly from 3 to 2 during the first 4 s of the simulation. The closed-loop time responses with K_{fir} and K_{fic} implemented are very similar. Note that no additional high-frequency dynamics were added in the nonlinear simulation to the original missile model. All controllers meet the desired performance goals.

VII. Conclusion

This paper presents formulas for synthesizing optimal FI, $\mathcal{H}_\infty$ controllers that directly account for real parametric LTV uncertainty. This procedure involves a linear matrix inequality, which may be solved using standard convex optimization methods. A missile autopilot is used to demonstrate the application of these methods. The direct inclusion of real parametric uncertainty into the control design procedure results in a 10–15% increase in robustness over controllers synthesized by treating the real parametric uncertainty as complex.

Appendix: State–Space Models and Controllers

This Appendix contains the continuous-time state–space representations of the missile and servomodels used in Fig. 2. The input to the servo is the commanded fin deflection in radian and the output is the actual fin deflection in radians:

$$\text{servo} = \left[\begin{array}{ccccc|c} -968 & -3.3\times10^7 & 0 & -1.4\times10^7 & 4.7\times10^7 & 0 \\ 0.0033 & 0 & 0 & 0 & 0 & 0 \\ 3.85 & 2.9\times10^6 & -1160 & -2.9\times10^6 & 0 & -1110 \\ & 0 & 1 & 0 & 0 & \end{array}\right]$$

The states of the missile are angle of attack in radian and pitch rate in radian/second. The first two inputs are the uncertainty associated with angle-of-attack, the next six are the uncertainty associated with Mach, and the final input is the fin deflection. The first two outputs are associated with angle-of-attack variations, the next six outputs with Mach variations, and the final output is the acceleration. Define the state–space missile model as

$$\left[\begin{array}{c|c} A_m & B_m \\ \hline C_m & D_m \end{array}\right]$$

where

$$\left[\begin{array}{c} A_m \\ \hline C_m \end{array}\right] = \left[\begin{array}{cc} -1.192 & 0.878 \\ 107.386 & -1.124 \\ \hline 26.546 & 0.000 \\ -13.898 & -0.001 \\ -5.182 & 0.004 \\ -11.294 & -0.017 \\ 13.367 & -0.005 \\ -9.550 & -0.001 \\ 0.269 & -0.003 \\ -0.392 & 0.002 \\ 100.373 & -0.071, \end{array}\right]$$

$$\left[\frac{B_m}{D_m}\right] = \left[\begin{array}{rrrrrrrrr} -0.007 & -0.014 & -0.008 & 0.001 & -0.014 & 0.034 & -0.041 & 0.009 & -0.202 \\ -13.896 & -26.542 & -85.768 & 8.577 & -0.210 & -0.432 & -0.223 & -0.106 & 221.668 \\ \hline 0.306 & -0.415 & 0.000 & 0.000 & -0.002 & 0.001 & 0.000 & 0.000 & 0.000 \\ 0.840 & -0.306 & -0.000 & -0.000 & 0.001 & -0.001 & -0.000 & -0.000 & -0.000 \\ 0.218 & 0.416 & 0.278 & 0.307 & 0.049 & 0.012 & 0.001 & -0.001 & -1.978 \\ 0.017 & 0.032 & -0.261 & -0.182 & 0.450 & 0.370 & 0.003 & 0.004 & 3.176 \\ 0.004 & 0.008 & -0.017 & -0.158 & 0.613 & -0.423 & -0.002 & -0.097 & 1.730 \\ -0.006 & -0.011 & 0.070 & -0.041 & 0.412 & -0.329 & -0.155 & 0.160 & 0.950 \\ -0.000 & -0.001 & 0.006 & 0.026 & 0.008 & 0.080 & 0.003 & 0.154 & 4.215 \\ 0.001 & 0.001 & -0.006 & -0.040 & -0.080 & -0.160 & 0.284 & -0.268 & 1.222 \\ -0.069 & -0.133 & -5.575 & -1.341 & 6.592 & -5.397 & 3.270 & 1.660 & 30.815 \end{array}\right]$$

The following matrices are the constant gain FI controllers. The first eight entries are gains for the state measurements, and the remaining gains are for the disturbance measurements. Note that the controller synthesized for systems with complex uncertainty K_{fic} is a state-feedback controller with real entries:

$$K_{\text{fic}} = \begin{bmatrix} -230.07 \\ -8.208 \\ -0.001 \\ -57.826 \\ 0.008 \\ 23.593 \\ -8.307 \\ 195.88 \end{bmatrix} \qquad K_{\text{fir}} = \begin{bmatrix} -0.007 + 0.000j \\ -0.091 + 0.001j \\ -0.164 + 0.011j \\ 0.300 + 0.028j \\ 0.265 + 0.028j \\ -0.173 + 0.034j \\ 0.021 + 0.031j \\ -2.739 - 0.031 \\ 0.011 + 0.000j \\ 0.021 + 0.000j \\ 0.053 + 0.001j \\ -0.004 - 0.000j \\ -0.006 + 0.000j \\ 0.005 - 0.000j \\ -0.003 + 0.000j \\ -0.002 + 0.000j \\ -0.553 + 0.005j \\ 0.002 - 0.000j \end{bmatrix}$$

The order of feedback measurements is given in Table A1.

Controller K_{fir} contains complex entries and can be realized as a real dynamic controller or real constant gain matrix using the techniques in Sec. V. The output feedback controller is a seven state controller. The inputs are the error between commanded and actual acceleration and the pitch rate; the output is commanded fin deflections in radian:

$$K_{\text{of}} = \left[\begin{array}{rrrrrrrrr} -67099.46 & -23241.21 & -1235.33 & 7633.90 & -4.31 & 9.38 & 123.41 & 0.43 & -579.91 \\ 0.00 & -2185.19 & -255.16 & 846.56 & -1.15 & 0.51 & 28.81 & 0.06 & -101.257 \\ 0.00 & 0.00 & -521.78 & -1761.67 & 0.33 & 0.12 & 14.99 & -0.02 & 27.36 \\ 0.00 & 0.00 & 1883.34 & -569.14 & -0.67 & -3.31 & 1.64 & 0.00 & 38.48 \\ 0.00 & 0.00 & 0.00 & 0.00 & -0.02 & -0.04 & 0.01 & 0.77 & -2.93 \\ 0.00 & 0.00 & 0.00 & 0.00 & 0.00 & -0.09 & 0.03 & -1.38 & 3.43 \\ 0.00 & 0.00 & 0.00 & 0.00 & 0.00 & 0.00 & -0.36 & 0.45 & 0.19 \\ \hline 580.09 & 110.16 & -12.76 & -6.32 & 4.39 & 1.83 & -0.53 & 0.00 & -0.07 \end{array}\right]$$

Table A1 Controller measurements

1	Missile state 1: angle-of-attack α, rad
2	Missile state 2: pitch rate q rad/s
3–6	Servo states
7	Performance weight state W_{perf}
8	Input uncertainty weight state W_{input}
9–10	Uncertainty parameter for angle of attack δ_α
11–16	Uncertainty parameter for Mach δ_M
17	Uncertainty parameter for input uncertainty δ_{input}
18	Commanded acceleration

Acknowledgments

The authors wish to acknowledge the generous financial support from the National Science Foundation (ECS-9110254), the NASA Langley Research Center (NAG-1-821), the Johns Hopkins University Applied Physics Laboratory (BPO-2229), the U.S. Naval Weapons Center (N60530-91-C-0218), and the University of Minnesota McKnight Land Grant Professorship.

References

'Doyle, J. C., Glover, K., Khargonekar, P. P., and Francis, B. A., "State-Space Solutions to Standard 3-12 and 34, Control Problems,'' *IEEE Transactions on Automatic Cantrol*, Vol. 34, No. 8, 1989, pp. 831–847.

[2]Doyle, J. C., "Structured Uncertainty in Control Design," *IEE Proceedings*, Vol. 129-D, No. 6, 1982, pp. 242–250.

[3]Haddad, W., and Bernstein, D., "Parameter-Dependent Lyapunov Functions, Constant Real Parameter Uncertainty, and the Popov Criterion in Robust Analysis and Synthesis," *Proceedings of the IEEE Conference on Decision and Control* (Brighton, England, UK), Inst. of Electrical and Electronics Engineers, New York, 1991, pp. 2274–2279.

[4]How, J. P., and Hall, S. R., "Application of Popov Controller Synthesis to Benchmark Problems with Real Parameter Uncertainty," *Journal of Guidance, Control, and Dynamics*, Vol. 17, No. 4, 1994, pp. 759–768.

'Young, P., "Robustness with Parametric and Dynamic Uncertainty," Ph.D. Thesis. Dept. of Electrical Engineering. California Inst. of Technology, Pasadena, CA, May 1993.

[6]Safonov, M. G., and Chiang, R. Y., "Real/Complex K_m-Synthesis Without Curve Fitting," *Control and Dynamical Systems*, Vol. 56, Academic, New York, 1993, pp. 303–324.

[7]Packard, A., Zhou, K., Pandey, P., Leonhardson, J., and Balas, G., "Optimal Constant I/O Similarity Scaling for Full Information and State Feedback Control Problems," *Systems and Control Letters*, Vol. 19, No. 4, 1992, pp. 271–280.

[8]Packard, A,, Zhou, K., Pandey, P., and Becker, G., "A Collection of Robust Control Problems Leading to LMIs," *Proceedings of the IEEE Conference on Decision and Control* (Brighton, England, UK), Inst. of Electrical and Electronics Engineers, New York, 1991, pp. 1245–1250.

[9]Packard, A., Doyle, J., and Balas, G., "Linear, Multivariable Robust

[13]Shamma, J., "Robust Stability with Time-Varying Structured Uncertainty," *IEEE Transactions on Automatic Control*, Vol. 39, No. 4, 1994, pp. 714–724.

[14]Rantzer, A., "Uncertainties with Bounded Rates of Variations," *Proceedings of the American Control Conference* (San Francisco, CA), Inst. of Electrical and Electronics Engineers, 1993, pp. 29, 30.

"Balas, G., Doyle, J., Glover, K., Packard, A., and Smith, R., "μ-Analysis and Synthesis Toolbox: Users Guide,'' MUSYN and Mathworks, Natick, MA, Dec. 1990.

[16]Lind, R., Balas, G., and Packard, A., "Robustness for LTI Systems in the Presence of LTV Real Parametric Uncertainty," *Proceedings of the American Control Conference* (Seattle, WA), Inst. of Electrical and Electronics Engineers, 1995, pp. 3463–3467.

[17]Reichert, R. T., "Robust Autopilot Design Using μ-Synthesis," *Proceedings of the American Control Conference* (San Diego, CA), Inst. of Electrical and Electronics Engineers, 1990, pp. 2368–2373.

[18]Ly, J., Safonov, M., and Ahmad, F., "Positive Real Parrott Theorem with Application to LMI Controller Synthesis," *Proceedings of the American Control Conference* (Baltimore, MD), Inst. of Electrical and Electronics Engineers, 1994, pp. 50–52.

"Boyd, S., El Ghaoui, L., Feron, E., and Balakrishnan, V., *Linear Matrix Inequalities in System and Control Theory*, SIAM Studies in Applied Mathematics, Society for Industrial and Applied Mathematics, Philadelphia, PA, 1994.

[20]Shor, N., *Minimization Methods for Non-Differentiable Functions*, Springer–Verlag, Berlin, 1985.

[21]Sontag, E., Rutgers Univ., New Brunswick, NJ, private communication, July 1994.

[22]Rotea, M., and Khargonekar, P., "Stabilization of Uncertain Systems with Norm Bounded Uncertainty—A Control Lyapunov Function Approach," *SIAM Journal on Control and Optimization*, Vol. 27, No. 6, 1989, pp. 1462–1476.

[23]Rotea, M., and Khargonekar, P., "Stabilizability of Linear Time-Varying and Uncertain Linear Systems," *IEEE Transactions on Automatic Control*, Vol. 33, No. 9, 1988, pp. 884–887.

[24]Balas, G., and Packard, A., "Development and Application of Time-Varying p-Synthesis Techniques for Control Design of Missile Autopilots,''Applied Physics Lab., Johns Hopkins Univ., Contract 605460-S (BPO-2229), Final Rept., Baltimore, MD, Jan. 1992.

[25]Balas, G., and Packard, A., "Design of Robust, Time-Varying Controllers for Missile Autopilots," *First IEEE Conference on Control Applications* (Dayton, OH), Inst. of Electrical and Electronics Engineers, 1992, pp. 172–178.

[26]Lind, R., Balas, G., and Packard, A., "Evaluating D-K Iteration for Control Design," *Proceedings of the American Control Conference* (Baltimore, MD), Inst. of Electrical and Electronics Engineers, 1994, pp. 2792–2797.